PHILOSOPHICAL TRANSACTIONS OF THE ROYAL SOCIETY A

rsta.royalsocietypublishing.org

Research

Cite this article: Sando D *et al*. 2014 Control of ferroelectricity and magnetism in multi-ferroic $BiFeO_3$ by epitaxial strain. *Phil. Trans. R. Soc. A* **372**: 20120438.
http://dx.doi.org/10.1098/rsta.2012.0438

One contribution of 10 to a Theme Issue 'Magnetoelectric phenomena and devices'.

Subject Areas:
solid state physics, materials science

Keywords:
multi-ferroics, $BiFeO_3$, Mössbauer spectroscopy, strain engineering

Author for correspondence:
M. Bibes
e-mail: manuel.bibes@thalesgroup.com

Control of ferroelectricity and magnetism in multi-ferroic $BiFeO_3$ by epitaxial strain

D. Sando[1], A. Agbelele[2], C. Daumont[1], D. Rahmedov[3], W. Ren[3], I. C. Infante[4], S. Lisenkov[5], S. Prosandeev[3], S. Fusil[1], E. Jacquet[1], C. Carrétéro[1], S. Petit[6], M. Cazayous[7], J. Juraszek[2], J.-M. Le Breton[2], L. Bellaiche[3], B. Dkhil[4], A. Barthélémy[1] and M. Bibes[1]

[1]Unité Mixte de Physique CNRS-Thales, 1 Av. A. Fresnel, 91767 Palaiseau, and Université Paris-Sud, 91405 Orsay, France
[2]Groupe de Physique des Matériaux, UMR6634 CNRS-Université de Rouen, 76801 St. Etienne du Rouvray, France
[3]Physics Department and Institute for Nanoscience and Engineering, University of Arkansas, Fayetteville, AR 72701, USA
[4]Laboratoire Structures, Propriétés et Modélisation des Solides, UMR 8580 CNRS-Ecole Centrale Paris, Grande Voie des Vignes, 92295 Châtenay-Malabry Cedex, France
[5]Department of Physics, University of South Florida, Tampa, FL 33647, USA
[6]Laboratoire Léon Brillouin, CEA/CNRS UMR12, 91191 Gif-sur-Yvette, France
[7]Laboratoire Matériaux et Phénomènes Quantiques (UMR 7162 CNRS), Université Paris Diderot-Paris 7, 75205 Paris cedex 13, France

Recently, strain engineering has been shown to be a powerful and flexible means of tailoring the properties of ABO_3 perovskite thin films. The effect of epitaxial strain on the structure of the perovskite unit cell can induce a host of interesting effects, these arising from either polar cation shifts or rotation of the oxygen octahedra, or both. In the multi-ferroic perovskite bismuth ferrite ($BiFeO_3$–BFO), both degrees of freedom exist, and thus a complex behaviour may be expected as one plays with epitaxial strain. In this paper, we review our results on the role

Royal Society Publishing

of strain on the ferroic transition temperatures and ferroic order parameters. We find that, while the Néel temperature is almost unchanged by strain, the ferroelectric Curie temperature strongly decreases as strain increases in both the tensile and compressive ranges. Also unexpected is the very weak influence of strain on the ferroelectric polarization value. Using effective Hamiltonian calculations, we show that these peculiar behaviours arise from the competition between antiferrodistortive and polar instabilities. Finally, we present results on the magnetic order: while the cycloidal spin modulation present in the bulk survives in weakly strained films, it is destroyed at large strain and replaced by pseudo-collinear antiferromagnetic ordering. We discuss the origin of this effect and give perspectives for devices based on strain-engineered $BiFeO_3$.

1. Introduction

Among multi-ferroics [1,2], $BiFeO_3$ (BFO) [3,4] has attracted a great deal of attention because of its high ferroic ordering temperatures (the Néel temperature T_N is 640 K and the ferroelectric Curie temperature T_C is 1100 K in the bulk) and large polarization (100 $\mu C\,cm^{-2}$ in high-quality single crystals [5] and thin films [6]). BFO crystallizes in the R3c space group, with cations polar-shifted along the pseudo-cubic ⟨111⟩ directions and FeO_6 octahedra rotated about the ⟨111⟩ axes. The magnetic order is antiferromagnetic G-type, with a superimposed cycloidal modulation with a long period of about 62 nm [7]. A magnetoelectric coupling between magnetic and ferroelectric orders has been demonstrated in films and single crystals. It allows the control of antiferromagnetic domains by an electric field [8,9], paving the way for low-power spintronics devices using multi-ferroics [2,4,10]. BFO has additional interesting virtues, such as a bandgap in the visible spectral range [11,12]—which may be useful for future photovoltaic devices [13–15]—conductive domain walls [16,17] and a high gating efficiency in ferroelectric field-effect structures [18].

The various functionalities of BFO are closely connected with the structural instabilities that coexist in this compound, and we describe in this paper our efforts to tune magnetism and ferroelectricity by means of strain engineering [19,20]. We have combined various experimental tools (temperature-dependent X-ray diffraction, neutron diffraction, piezoresponse force microscopy (PFM) and Mössbauer spectroscopy) with effective Hamiltonian calculations. As a series of examples, we report the influence of strain on the ferroic phase transitions, the ferroelectric polarization and the magnetic order.

2. Sample elaboration

To conduct a detailed study on the numerous properties of BFO and their response to epitaxial strain, a series of films on various substrates imposing a range of misfit strains from −2.5% to +1.3% were grown by pulsed laser deposition [21–23]. The substrates used were (La, Sr)(Al, Ta)O_3 (LSAT), $SrTiO_3$ (STO), $DyScO_3$ (DSO), $GdScO_3$ (GSO), $SmScO_3$ (SSO), $NdScO_3$ (NSO) and $PrScO_3$ (PSO). The scandates were (110)-oriented (orthorhombic notation) while the cubic LSAT and STO were (001)-oriented. Note that we use pseudo-cubic notation throughout this paper. All films had a nominal thickness of 70 nm, except the one deposited on LSAT for which the thickness was 35 nm. X-ray $2\theta/\omega$-scans and reciprocal space maps [24] showed that the films were grown in a single epitaxial phase and were fully strained. For Mössbauer spectroscopy experiments, the BFO target used for sample preparation was 100% enriched with ^{57}Fe. Lower electrodes of $SrRuO_3$ or (La,Sr)MnO_3 were intercalated between the substrate and BFO film for transport and ferroelectric property measurements. To perform electrical characterization measurements, we used targets of BFO doped with 5% Mn to reduce leakage [25,26]. Gold top electrodes, 10–50 μm in diameter, were deposited using DC sputtering and lift-off.

3. Strain and ferroic transition temperatures

First, we investigated the effect of strain on the ferroelectric T_C of the films. For this, we combined temperature-dependent X-ray diffraction with PFM measurements. As the films are completely strained, the out-of-plane (OP) lattice parameter can be used as an indicator of structural and phase transitions in BFO. We measured the OP c lattice parameter of the film and the substrate and its dependence on temperature. We found that while the substrate c parameter exhibited a linear trend from thermal expansion, the BFO c parameter displayed an inflection point at temperatures that varied for the different samples. From this inflection point, the Curie temperature of the films was deduced [24].

To complement the X-ray measurements, we characterized the ferroelectric response of the films using PFM. Here, ferroelectric domains were written in the BFO using a conductive atomic force microscope tip by applying a DC voltage between the tip and lower electrode. The samples were then heated under an oxygen atmosphere at a target temperature for 2 h. After the annealing process, PFM at room temperature was used to image the previously written domain structure. For the strongly compressively strained samples, the domains were destroyed at progressively lower temperatures as the strain increased. This confirms that the T_C of the films is indeed reduced with increasing compressive strain.

The Néel temperature T_N of the films was determined for selected samples by means of temperature-dependent neutron diffraction and Mössbauer spectroscopy. For the neutron diffraction experiments, we used the BFO//STO sample, and the intensity of the atomic force microscope peak $(1/2\ 1/2\ 1/2)_c$ was monitored as a function of temperature. A decrease in the intensity of this peak at around 570 K signified a change in the magnetic state of the sample, leading us to deduce a Néel temperature around 570 K for this film. From temperature-dependent Mössbauer spectroscopy measurements, we measured the hyperfine field [27] in our BFO//GSO sample and found that this hyperfine field decreased with increasing temperature to extrapolate to zero at 640 K, a temperature we take as T_N. In bulk BFO, the temperature dependence of the OP parameter c shows a step at T_N. In our films, we could also detect a slight change of slope in the c versus T data in the 600–650 K range.

The T_C and T_N values for all films are summarized in the phase diagram in figure 1, together with results from first-principles-based effective Hamiltonian (Heff) calculations (taking into account both the antiferrodistortive angles—that is, the oxygen-octahedra rotations—and the cation shifts). The calculations [28] were performed at 300 K to gain insight into the observed T_C and T_N trends with misfit strain. In figure 1*a*,*b*, we plot the Heff-computed tetragonality (c/a ratio) and the rotation angles of the oxygen octahedra about the x-, y- and z-axes. The tetragonality increases with increasing (compressive) strain, as expected, and the rotation angles also vary quite substantially. In perovskites, polar and rotational degrees of freedom usually exclude each other, i.e. rotations are detrimental to polar shifts and thus to ferroelectricity. In BFO, however, both degrees of freedom are present, and our calculations indicate that while strain tends to elongate the unit cell (which in a conventional tetragonal ferroelectric would increase polar shifts and strengthen ferroelectricity) it also considerably enhances the rotation angles. Both the experimental and theoretical data show a strong decrease in T_C versus strain, which indicates that the strain-induced increase in the octahedra tilts is the main factor driving the ferroelectric response in BFO films. Also reproduced by theory is the weak dependence of the T_N on strain, consistent with the variation of the Fe–O–Fe bond angles by a few degrees, and its influence of super-exchange interactions for large bond angles [29] (i.e. far from the crossover between antiferromagnetic and ferromagnetic exchange that occurs at around 127°). For compressive strains higher than about 3%, we predict that T_C and T_N will eventually coincide, which might lead to an enhanced magnetoelectric response. However, experimentally it remains a challenge to stabilize R-type BFO at such strain levels, as crystallization in a T-type polymorph [30] becomes increasingly favourable [31–33].

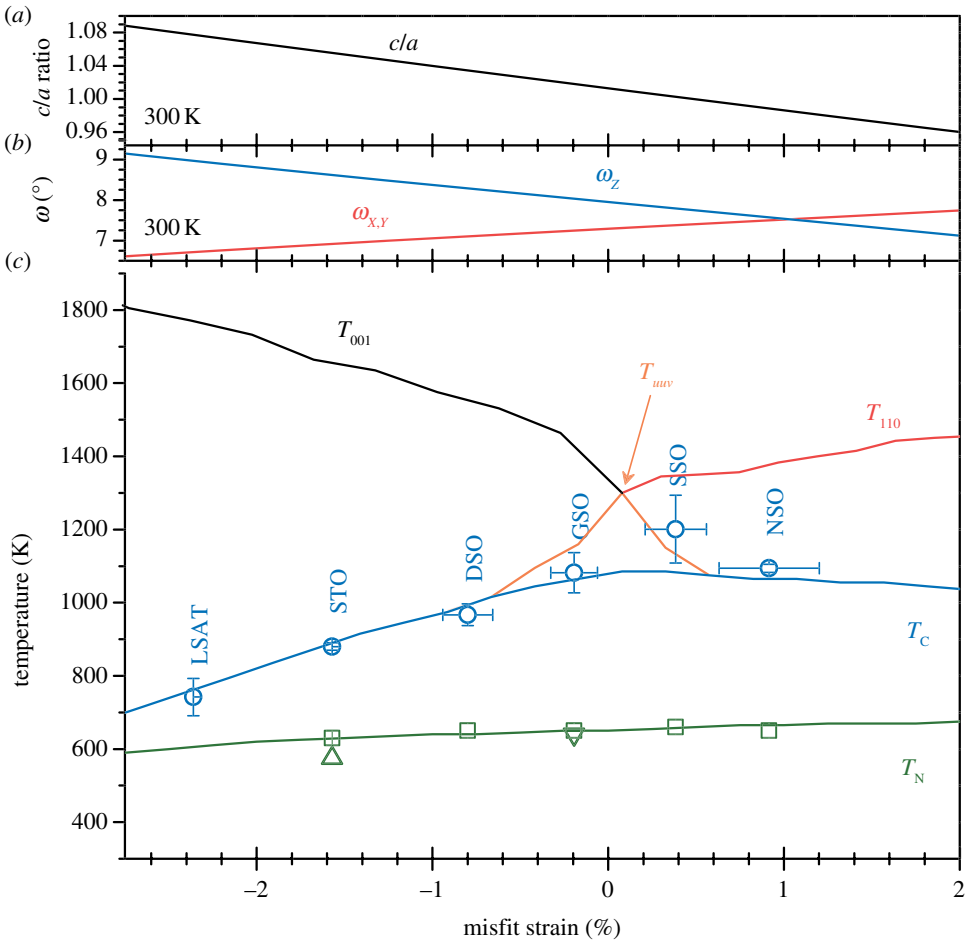

Figure 1. Effective Hamiltonian results evaluated in a BFO film, at 300 K and as a function of misfit strain; (*a*) tetragonality (*c*/*a* ratio) and (*b*) antiferrodistortive angles ω along the *x*-, *y*- and *z*-axes (ω_X and ω_Y, red line and ω_Z, blue line). (*c*) Theoretical results on BFO film transition temperatures as a function of misfit strain. The activation temperatures for the antiferrodistortive oxygen tilting along the *z*-direction (tetragonal distortion T_{001}, black line), for the antiferrodistortive oxygen tilting within the *x*–*y* plane (orthorhombic distortion T_{110}, red line), and for the tilting along a [*uuv*] direction (monoclinic distortion T_{uuv}, orange line) are also plotted. Experimental T_C (circles) and T_N (squares and triangles) values. Vertical error bars for T_N values correspond to symbol size and for T_C values result from maximum variation of T_C that may be obtained between different fitting processes using the mean field function. Below T_C, for any considered strain, the simulations predict that the crystallographic phase is Cc, with a polarization along a [*uuv*] direction while the oxygen octahedra rotate about a [$u'u'v'$] axis. Adapted from [24]. (Online version in colour.)

4. Strain and polarization

In order to gain an understanding of how the ferroelectric polarization is modified by epitaxial strain, we measured $I(V)$ loops using an Aixacct TF Analyzer 2000 at 1 kHz. The *I*–*V* curves were corrected for leakage and time integrated to yield polarization *P*–*E* loops for each sample. From the polarization loops, the coercive voltage and remanent polarization were extracted [34]. The behaviour of the spontaneous polarization with epitaxial strain is presented in figure 2. Here, we compare the experimental results with first-principles calculations, where the agreement between measured and calculated trends is quite good. In measuring the remanent polarization in $(001)_{pc}$

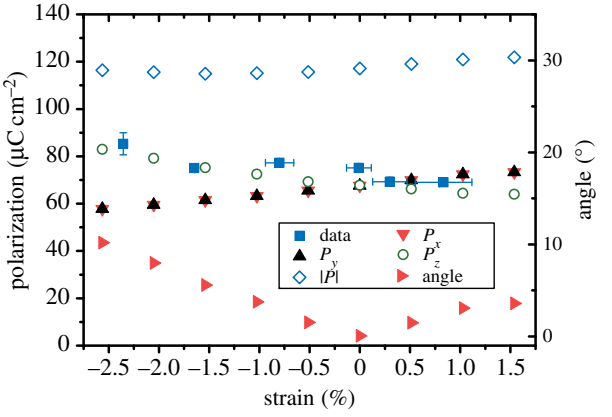

Figure 2. Measured (squares) remanent polarization versus strain and calculated components of the remanent polarization vector. The norm of the polarization vector and the angle this vector makes with the ⟨111⟩ direction are also shown. Adapted from [34]. (Online version in colour.)

samples, we are in fact measuring the projection of the polarization (which usually lies along a ⟨111⟩ direction) along the ⟨001⟩ direction. Thus, any rotation in the polarization vector towards (respectively away from) the in-plane direction will induce a decrease (respectively increase) in the measured remanent polarization. This observation is consistent with the results presented here, i.e. the total polarization is hardly changed by strain.

5. Strain and magnetic ordering

Finally, we have explored the effect of epitaxial strain on the cycloidal spin order present in the bulk. Previous neutron diffraction studies have indicated that the cycloid is absent for films grown on $SrTiO_3$ (compressive strain of 1.6%) [35]. However, subsequent experiments on thicker films did evidence cycloidal ordering [36], whose presence was ascribed to the relaxed structure of the films owing to their larger thickness (200 nm versus 70 nm in [35]). These results are, at least qualitatively, consistent with the predictions of Bai *et al.* [37] that an epitaxial strain of about 1% would make the cycloid unstable against a (pseudo-collinear) antiferromagnetic order.

To revisit the role of strain on magnetic order, we conducted conversion electron Mössbauer spectroscopy (CEMS) measurements on our strain series of films. The experiments were performed using a γ-ray beam from an approximately 50 mCi ^{57}Co radioactive source under normal incidence, and the conversion electrons were collected using a homemade He–CH_4 gas flow proportional counter [38].

The room temperature Mössbauer spectra of the BFO//GSO and BFO//PSO samples are presented in figure 3. Both spectra exhibit a six-line magnetic hyperfine pattern with an isomer shift value of 0.37 mm s^{-1} (relative to α-Fe at 295 K) corresponding to the trivalent state of iron ions in the octahedral positions.

The Mössbauer spectrum of the film on GSO (figure 3*a*) exhibits inhomogeneous line broadenings with a clear asymmetry, very similar to the case of bulk BFO with a cycloidal spin structure. It has been shown that such a spectral asymmetry in BFO can be explained by a slight modulation of the excited states' hyperfine energies, arising when (i) the hyperfine field rotates by an angle θ with respect to the principal axis OZ of the electric field gradient tensor and (ii) such a rotation leads to an anisotropic variation of the hyperfine field magnitude [5]. In a single-crystal spectrum, this rotation will also change the line intensity ratio R_{23} between the second (or fifth) and third (or fourth) lines on the magnetic hyperfine sextet, which depends on the angle β between the Fe spin and the incident γ-ray direction.

Assuming that OZ is along the polarization direction [111], we modelled the Mössbauer spectrum of BFO on GSO using a correlated distribution of the quadrupole shift

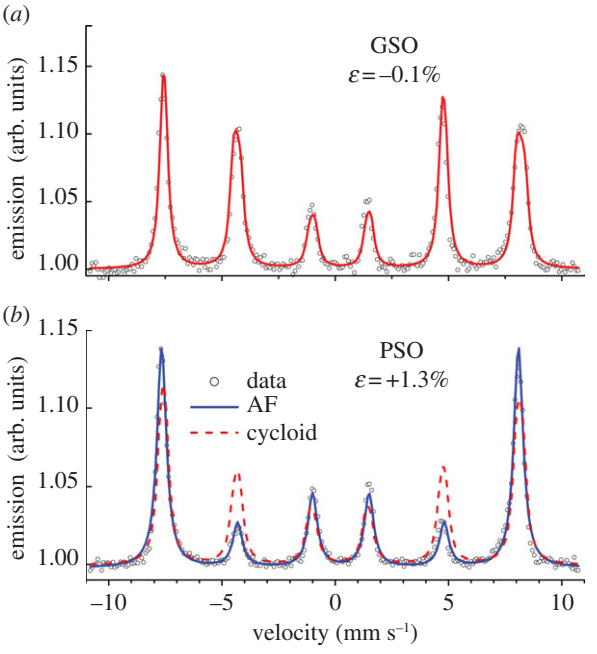

Figure 3. Conversion electron Mössbauer spectra at 295 K for two BFO films; (*a*) one on GSO and (*b*) the other on PSO. The symbols correspond to the data, the red lines to a fit with a cycloidal model and the blue line to a fit with an antiferromagnetic (AF) order. Adapted from [39]. (Online version in colour.)

$2\epsilon(\theta) = -\Delta E_Q/2(3\cos^2\theta - 1)$, where $\Delta E_Q = 0.44\,\mathrm{mm\,s^{-1}}$ is the quadrupole coupling parameter, $B_{\mathrm{hf}}(\theta) = B_{\mathrm{hf}//}\cos^2\theta + B_{hf\perp}\sin^2\theta$ and $R_{23}(\theta) = 4[1-\cos^2\beta(\theta)]/[1+\cos^2\beta(\theta)]$, as θ rotates into the (111) plane containing *OZ* in the cycloidal magnetic structure. It can be seen that the experimental data are very well reproduced with an asymmetry parameter $h = B_{\mathrm{hf}//}/B_{\mathrm{hf}\perp} = 0.98$.

For the film on PSO (figure 3*b*), the CEMS spectrum has a symmetric shape with a very low intensity of the second and third lines, evidencing a preferred OP orientation of the Fe antiferromagnetic moments. A fit by a cycloidal spin arrangement model is not applicable in this case, even with a vertical plane of the cycloid, as shown in figure 3*b*. The data were therefore fitted using a single hyperfine sextet as expected in the case of a collinear spin structure. A hyperfine field value of 49 T, close to the bulk BFO value, and average angle $\beta = 28^\circ$ between the Fe spins and incident γ-ray radiation were extracted from the fit.

We thus conclude that, at high tensile strain, the cycloidal spin structure is destroyed and an OP orientation of the spins is obtained, while for BFO on substrates that impose a small strain, the cycloid survives.

6. Conclusion

In summary, we have reported the influence of epitaxial strain on the ferroic properties of multiferroic $BiFeO_3$ thin films. The coexistence of the polar and tilting structural instabilities yields a peculiar behaviour, completely different from that observed in classical ferroelectrics, such as $PbTiO_3$ or $BaTiO_3$. Indeed, in BFO we find that the Curie temperature strongly *decreases* with strain, and that there is little change in the polarization. Using first-principles-based calculations, we show that this is due to the dominant influence of oxygen-octahedra rotations, whose strain-induced amplification tends to destabilize ferroelectricity. We have also investigated the role of strain on magnetic order. While we confirm the presence of a bulk-like cycloidal spin arrangement in weakly strained films (on $GdScO_3$), a strong tensile strain (using $PrScO_3$ substrates) destroys

the cycloid and favours a pseudo-collinear antiferromagnetic ordering, as had been found earlier for strong compressive strain (using $SrTiO_3$). Thus, strain engineering appears to be an interesting approach to unveil new properties and phenomena in $BiFeO_3$. We anticipate more surprises by extending this study to other functionalities, for instance in optics. In terms of potentisal device applications, using piezoelectric substrates could allow controlling ferroic orders by an electric field, following the already observed control of polarization amplitude and coercive voltage [40].

Acknowledgement. We are grateful to D. Colson for providing the ^{57}Fe-enriched target.

Funding statement. Financial support from the French Agence Nationale de la Recherche (ANR) through projects NOMILOPS and MULTIDOLLS is acknowledged. The computational works were supported by an NSF DMR-1066158 grant (D.R. and L.B.), ARO grant W911NF-12-1-0085 (W.R. and L.B.) and the Office of Naval Research, under grants N00014-11-1-0384 and N00014-12-1-1034 (S.P. and L.B.).

References

1. Eerenstein W, Mathur ND, Scott JF. 2006 Multiferroic and magnetoelectric materials. *Nature* **442**, 759–765. (doi:10.1038/nature05023)
2. Bibes M, Villegas JE, Barthélémy A. 2011 Ultrathin oxide films and interfaces for electronics and spintronics. *Adv. Phys.* **60**, 5–84. (doi:10.1080/00018732.2010.534865)
3. Catalan G, Scott JF. 2009 Physics and applications of bismuth ferrite. *Adv. Mater.* **21**, 2463–2485. (doi:10.1002/adma.200802849)
4. Béa H, Gajek M, Bibes M, Barthélémy A. 2008 Spintronics with multiferroics. *J. Phys. Condens. Matter* **20**, 434221. (doi:10.1088/0953-8984/20/43/434221)
5. Lebeugle D, Colson D, Forget A, Viret M, Bonville P, Marucco JF, Fusil S. 2007 Room-temperature coexistence of large electric polarization and magnetic order in $BiFeO_3$ single crystals. *Phys. Rev. B* **76**, 024116. (doi:10.1103/PhysRevB.76.024116)
6. Béa H, Bibes M, Zhu X-H, Fusil S, Bouzehouane K, Petit S, Kreisel J, Barthélémy A. 2008 Crystallographic, magnetic, and ferroelectric structures of bulklike $BiFeO_3$ thin films. *Appl. Phys. Lett.* **93**, 072901. (doi:10.1063/1.2940327)
7. Sosnowska I, Peterlin-Neumaier T, Steichele E. 1982 Spiral magnetic ordering in bismuth ferrite. *J. Phys. C* **15**, 4835–4846.
8. Zhao T *et al.* 2006 Electrical control of antiferromagnetic domains in multiferroic $BiFeO_3$ films at room temperature. *Nat. Mater.* **5**, 823–829. (doi:10.1038/nmat1731)
9. Lebeugle D, Colson D, Forget A, Viret M, Bataille AM, Gukasov A. 2008 Electric-field-induced spin flop in $BiFeO_3$ single crystals at room temperature. *Phys. Rev. Lett.* **100**, 227602. (doi:10.1103/PhysRevLett.100.227602)
10. Bibes M. 2012 Nanoferronics is a winning combination. *Nat. Mater.* **11**, 354–357. (doi:10.1038/nmat3318)
11. Kumar A *et al.* 2008 Linear and nonlinear optical properties of $BiFeO_3$. *Appl. Phys. Lett.* **92**, 121915. (doi:10.1063/1.2901168)
12. Allibe J *et al.* 2010 Optical properties of integrated multiferroic $BiFeO_3$ thin films for microwave applications. *Appl. Phys. Lett.* **96**, 182902. (doi:10.1063/1.3402763)
13. Choi T, Lee S, Choi YJ, Kiryukhin V, Cheong S-W. 2009 Switchable ferroelectric diode and photovoltaic effect in $BiFeO_3$. *Science* **324**, 63–6. (doi:10.1126/science.1168636)
14. Seidel J, Fu D, Yang S-Y, Alarcón-Lladó E, Wu J, Ramesh R, Ager J. 2011 Efficient photovoltaic current generation at ferroelectric domain walls. *Phys. Rev. Lett.* **107**, 126805. (doi:10.1103/PhysRevLett.107.126805)
15. Kreisel J, Alexe M, Thomas PA. 2012 A photoferroelectric material is more than the sum of its parts. *Nat. Mater.* **11**, 260. (doi:10.1038/nmat3282)
16. Seidel J *et al.* 2009 Conduction at domain walls in oxide multiferroics. *Nat. Mater.* **8**, 229–234. (doi:10.1038/nmat2373)
17. Farokhipoor S, Noheda B. 2011 Conduction through 71° domain walls in $BiFeO_3$ thin films. *Phys. Rev. Lett.* **107**, 127601. (doi:10.1103/PhysRevLett.107.127601)
18. Crassous A *et al.* 2011 Nanoscale electrostatic manipulation of magnetic flux quanta in ferroelectric/superconductor $BiFeO_3/YBa_2Cu_3O_{7-\delta}$ heterostructures. *Phys. Rev. Lett.* **95**, 247002. (doi:10.1103/PhysRevLett.107.247002)
19. Choi K *et al.* 2004 Enhancement of ferroelectricity in strained $BaTiO_3$ thin films. *Science* **306**, 1005–1009. (doi:10.1126/science.1103218)

20. Schlom DG, Chen L-Q, Eom C-B, Rabe KM, Streiffer SK, Triscone J-M. 2007 Strain tuning of ferroelectric thin films. *Annu. Rev. Mater. Res.* **37**, 589–626. (doi:10.1146/annurev.matsci.37.061206.113016)
21. Béa H *et al.* 2005 Influence of parasitic phases on the properties of $BiFeO_3$ epitaxial thin films. *Appl. Phys. Lett.* **87**, 072508. (doi:10.1063/1.2009808)
22. Béa H *et al.* 2006 Combining half-metals and multiferroics into epitaxial heterostructures for spintronics. *Appl. Phys. Lett.* **88**, 062502. (doi:10.1063/1.2170432)
23. Zhu XH *et al.* 2008 Thickness-dependent structural and electrical properties of multiferroic Mn-doped $BiFeO_3$ thin films grown epitaxially by pulsed laser deposition. *Appl. Phys. Lett.* **93**, 082902. (doi:10.1063/1.2969785)
24. Infante I *et al.* 2010 Bridging multiferroic phase transitions by epitaxial strain in $BiFeO_3$. *Phys. Rev. Lett.* **105**, 057601. (doi:10.1103/PhysRevLett.105.057601)
25. Singh SK, Ishiwara H, Maruyama K. 2006 Room temperature ferroelectric properties of Mn-substituted $BiFeO_3$ thin films deposited on Pt electrodes using chemical solution deposition. *Appl. Phys. Lett.* **88**, 262908. (doi:10.1063/1.2218819)
26. Singh SK, Menou N, Funakubo H, Maruyama K, Ishiwara H. 2007 (111)-textured Mn-substituted $BiFeO_3$ thin films on $SrRuO_3/Pt/Ti/SiO_2/Si$ structures. *Appl. Phys. Lett.* **90**, 212914. (doi:10.1063/1.2748323)
27. De Sitter J, Dauwe C, De Grave E, Govaert A. 1976 On the Mössbauer parameters in $BiFeO_3$. *Solid State Commun.* **18**, 645–646. (doi:org/10.1016/0038-1098(76)91502-7)
28. Kornev I, Lisenkov S, Haumont R, Dkhil B, Bellaiche L. 2007 Finite-temperature properties of multiferroic $BiFeO_3$. *Phys. Rev. Lett.* **99**, 227602. (doi:10.1103/PhysRevLett.99.227602)
29. Seo JW, Fullerton EE, Nolting F, Scholl A, Fompeyrine J, Locquet J-P. 2008 Antiferromagnetic $LaFeO_3$ thin films and their effect on exchange bias. *J. Phys. Condens. Matter* **20**, 264014. (doi:10.1088/0953-8984/20/26/264014)
30. Béa H *et al.* 2009 Evidence for room-temperature multiferroicity in a compound with a giant axial ratio. *Phys. Rev. Lett.* **102**, 217603. (doi:10.1103/PhysRevLett.102.217603)
31. Dupé B *et al.* 2010 Competing phases in $BiFeO_3$ thin films under compressive epitaxial strain. *Phys. Rev. B* **81**, 144128. (doi:10.1103/PhysRevB.81.144128)
32. Hatt AJ, Spaldin NA. 2010 Strain-induced isosymmetric phase transition in $BiFeO_3$. *Phys. Rev. B* **81**, 054109. (doi:10.1103/PhysRevB.81.054109)
33. Wojdel J, Íñiguez J. 2010 *Ab initio* indications for giant magnetoelectric effects driven by structural softness. *Phys. Rev. Lett.* **105**, 037208. (doi:10.1103/PhysRevLett.105.037208)
34. Daumont C *et al.* 2012 Strain dependence of polarization and piezoelectric response in epitaxial $BiFeO_3$ thin films. *J. Phys. Condens. Matter.* **24**, 162202. (doi:10.1088/0953-8984/24/16/162202)
35. Béa H, Bibes M, Petit S, Kreisel J, Barthélémy A. 2007 Structural distortion and magnetism of $BiFeO_3$ epitaxial thin films: a Raman spectroscopy and neutron diffraction study. *Philos. Mag. Lett.* **87**, 165–174. (doi:10.1080/09500830701235802)
36. Ke X, Zhang P, Baek S, Zarestky J, Tian W, Eom C. 2010 Magnetic structure of epitaxial multiferroic $BiFeO_3$ films with engineered ferroelectric domains. *Phys. Rev. B* **82**, 134448. (doi:10.1103/PhysRevB.82.134448)
37. Bai F, Wang J, Wuttig M, Li J, Wang N, Pyatakov AP, Zvezdin AK, Cross LE, Viehland D. 2005 Destruction of spin cycloid in $(111)_c$-oriented $BiFeO_3$ thin films by epitiaxial constraint: enhanced polarization and release of latent magnetization. *Appl. Phys. Lett.* **86**, 032511. (doi:10.1063/1.1851612)
38. Juraszek J, Zivotsky O, Chiron H, Vaudolon C, Teillet J. 2009 A setup combining magneto-optical Kerr effect and conversion electron Mössbauer spectrometry for analysis of near-surface properties of thin films. *Rev. Sci. Instrum.* **80**, 043905. (doi:10.1063/1.3121215)
39. Sando D *et al.* 2013 Crafting the magnonic and spintronic response of $BiFeO_3$ films by epitaxial strain. *Nature Mater.* **12**, 641–646. (doi:10.1038/nmat3629).
40. Biegalski MD, Kim DH, Choudhury S, Chen LQ, Christen HM, Dörr K. 2011 Strong strain dependence of ferroelectric coercivity in a $BiFeO_3$ film. *Appl. Phys. Lett.* **98**, 142902. (doi:10.1063/1.3569137)